Chinese Chemical Letters 33 (2022) 4313–4316

Contents lists available at ScienceDirect

Chinese Chemical Letters

journal homepage: www.elsevier.com/locate/cclet

Efficient dye-sensitized solar cells based on concerted companion dyes: Systematic optimization of thiophene units in the organic dye components

Jiaxin Luo[1], Zhengli Xie[1], Jiazhi Zou, Xinyan Wu*, Xueqing Gong*, Chengjie Li*, Yongshu Xie*

Key Laboratory for Advanced Materials and Institute of Fine Chemicals, Centre for Computational Chemistry and Research Institute of Industrial Catalysis, School of Chemistry and Molecular Engineering, East China University of Science and Technology, Shanghai 200237, China

ARTICLE INFO

Article history:
Received 19 November 2021
Revised 17 January 2022
Accepted 18 January 2022
Available online 23 January 2022

Keywords:
Dye sensitized solar cells
Concerted companion dyes
Porphyrin dyes
Cosensitization

ABSTRACT

To develop efficient concerted companion (CC) dyes for fabricating high-performance DSSCs, three organic dyes **XL1**-**XL3** have been designed by varying the position and number of the β-hexylthiophene (HT) bridges, and these organic dye units are covalently linked with our previously reported porphyrin dye **XW10** to construct the corresponding CC dyes **XW74**-**XW76**. Among the organic dyes, **XL3** contains two β-hexylthiophene units at both the donor and acceptor parts and thus possesses stronger light-harvesting capability in the green light region. Because of the most complementary absorption between **XL3** and **XW10** as well as the excellent photovoltaic behavior of the individual **XL3** dye, the corresponding CC dye **XW76** affords the best PCE (10.78%) among all the CC dyes. Upon coadsorption with CDCA, **XW76** affords a highest PCE of 11.35%, which outperforms the previous cosensitization system of **XW10**+**WS-5**. This work provides an approach for developing efficient DSSCs based on CC dyes composed of an organic dye unit with suitable π spacers inserted at appropriate positions.

Among the third-generation photovoltaic devices, dye-sensitized solar cells (DSSCs) have aroused considerable attention owing to their easy fabrication and colorful appearance since the first report by Grätzel and O'Regan in 1991 [1–3]. The power conversion efficiencies (PCE) have been dramatically promoted with the development of various mesoscopic semiconductors [4], photosensitizers [5], redox shuttles [6,7] and device designs [8,9]. Among them, the photoactive sensitizers act as the electron pumps to harvest light and transfer the excited electrons into the semiconductor in the DSSCs. In this respect, various types of sensitizers have been developed. For example, ruthenium-based complexes [10], metal-free organic dyes [11–13] and zinc porphyrin dyes [14–18] have been designed to enhance the PCEs [19–25].

Porphyrin sensitizers, as the analogues of chlorophylls in photosynthesis, possess the properties of intense and broad absorption, convenient modification and remarkable light-thermal stability, which enable them to be effective in fabricating efficient DSSCs [26,27]. However, the absorption valley for porphyrins in the green light region limits their light-harvesting capability and the related photovoltaic performance [28,29].

To fill up the absorption valley and improve the PCEs, various organic sensitizers have been designed and used as the cosensitizers for porphyrins to fabricate efficient DSSCs [18,30]. However, a number of factors need to be optimized for fabricating the cosensitized DSSC devices, and the distribution of the dyes on the semiconductor is rather difficult to control, which is unfavorable for further improving the photovoltaic performance [31]. To address these problems, we have recently developed a novel class of concerted companion (CC) dyes to achieve the "intramolecular cosensitization" effect by covalently linking the organic dye and porphyrin dye units through long chains [14,32]. Remarkably, such dyes feature panchromatic absorption, and endow the corresponding DSSCs with high-efficiency and long-term photostability. Based on this background, we herein report the optimization of the organic dyes to systematically modulate the absorption and thus improve the performance of CC dyes. With respect to the design of organic dyes, the thiophene unit has been extensively used as the π spacer [33], and its number [34,35] and position [36,37] in the dye framework dramatically affect the photophysical properties of the sensitizers. Thus, three organic dyes **XL1**-**XL3** have been synthesized by incorporating the β-hexylthiophene (HT) unit as the π

* Corresponding authors.
E-mail addresses: xinyanwu@ecust.edu.cn (X. Wu), xgong@ecust.edu.cn (X. Gong), chengjie.li@ecust.edu.cn (C. Li), yshxie@ecust.edu.cn (Y. Xie).
[1] These authors contributed equally to this work.

https://doi.org/10.1016/j.cclet.2022.01.052
1001-8417/

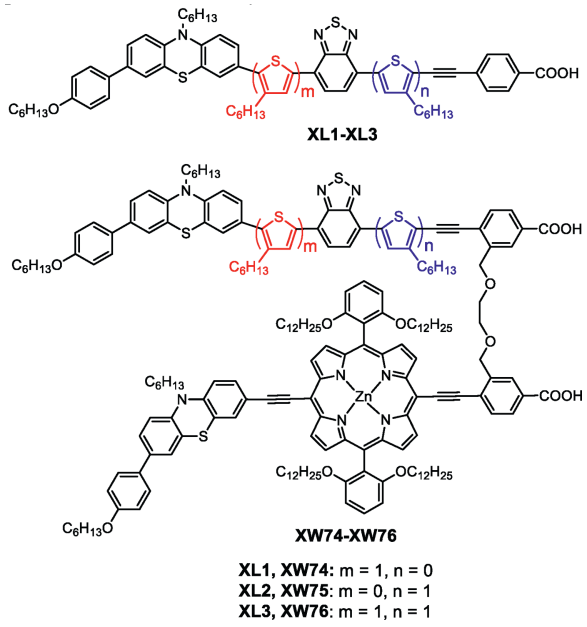

Fig. 1. Molecular structures of dyes **XL1**-**XL3, XW74**-**XW76**.

spacer, the electron-rich phenothiazine unit as the donor [38,39], and benzothiadiazole as the auxiliary acceptor [40]. Then, these organic dye units are covalently linked with our previously reported porphyrin dye **XW10** [20] to construct the corresponding CC dyes **XW74**–**XW76** (Fig. 1).

The number and position of the HT units dramatically affect the photovoltaic behaviors of **XL1**–**XL3**. When it is shifted from the donor (**XL1**) to the acceptor side (**XL2**), the anti-aggregation and recombination suppressing capability are obviously improved, accompanied with the elongation of the electron lifetime, giving rise to an improved V_{OC} (819 mV) for **XL2**. On the other hand, dye **XL3** contains two HT units at both sides of the benzothiadiazole unit, and it not only shows stronger absorption in the green light region, but also keeps the well-defined anti-aggregation character. As a result, broadened IPCE profile, improved J_{SC}, high V_{OC} and a relatively high PCE of 8.69% have been obtained for **XL3**. Because of the most complementary absorption character between **XL3** and **XW10** as well as the good photovoltaic behavior for the individual **XL3** dye, the corresponding CC dye **XW76** affords the highest J_{SC}, V_{OC} and PCE (10.78%) among the CC dyes. Notably, further coadsorption with chenodeoxycholic acid (CDCA) affords a high PCE of 11.35%. This work illustrates the importance of tailoring the position and number of π spacers in the organic dye components for regulating the spectral response and thus elevating the photovoltaic performance of the CC dyes.

The synthetic procedures for **XL1**–**XL3** and **XW74**–**XW76** are illustrated in Scheme S1 (Supporting information). The dye precursors were obtained *via* Sonogashira and Suzuki coupling reactions. Subsequent hydrolysis reactions under alkali conditions afforded the final dyes. The structures of all new compounds have been characterized by NMR and mass spectra, see details in Supporting information.

Fig. 2 presents the absorption spectra of the dyes in THF and adsorbed on thin TiO_2 films, and Table S1 (Supporting information) summarizes the corresponding data. The different positions of the HT unit in the isomeric dyes **XL1** and **XL2** induce a 16 nm red shift of the low energy transition band for **XL2** (494 nm) relative to that of **XL1** (478 nm), demonstrating that the thiophene moiety linked neighboring to the acceptor unit may induce less distortion and better conjugation of the molecule [41], as indicated by the calculated smaller dihedral angles in the optimized structures (*vide infra*). Different from these two dyes, **XL3** contains two HT units on both sides of the benzothiadiazole unit, exhibiting a further bathochromically shifted absorption peak at 507 nm with a higher molar extinction coefficient. Compared with **XL1** and **XL2, XL3** is expected to be a better cosensitizer for porphyrin dye **XW10**, considering its better compensation of the absorption valley of **XW10**. Indeed, by combining **XL3** with **XW10**, the CC dye **XW76** presents a better panchromatic response compared to **XW74** and **XW75**, especially in the wavelength range from 500 nm to 600 nm (Fig. 2a).

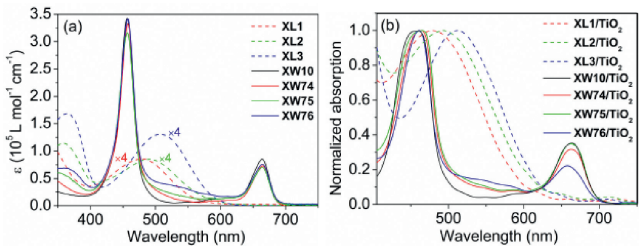

Fig. 2. Absorption spectra of the sensitizers (a) in THF solutions, and (b) adsorbed on TiO_2 films (2 μm).

Upon adsorption onto the TiO_2 films (Fig. 2b), **XL1**–**XL3** and **XW74**–**XW76** show broadened bands, which facilitate the light harvesting in the DSSCs. Notably, the absorption spectra exhibit negligible blue shift upon adsorption, compared with those in the solutions, indicating the absence of notable aggregation on the TiO_2 films [32].

Electrochemical behavior of the organic dyes and CC dyes adsorbed on TiO_2 films were measured by cyclic voltammetry (CV) and differential pulse voltammetry (DPV) (Table S2, Figs. S2 and S3 in Supporting information) to evaluate the feasibility of electron transfer. The highest occupied molecular orbital (HOMO) levels of **XL1**–**XL3** and **XW74**–**XW76** are 0.95∼0.99 V *vs.* NHE, more positive than the I^-/I_3^- redox potential (∼0.4 V *vs.* NHE), indicating the possibility for dye regeneration. In addition, their lowest unoccupied molecular orbital (LUMO) levels are calculated to be −1.26 ∼ −0.94 V *versus* NHE, well above the conduction band edge of TiO_2 (−0.5 V *vs.* NHE), implying the feasibility for electron injection.

The two sub-dye units in the CC dyes are expected to be electronically independent, as have been revealed by the theoretical calculations in our previous work [32]. Herein, we have investigated the optimized molecule structures and the frontier molecular orbitals of the **XL** dyes using DFT calculations [42]. As presented in Fig. S4 (Supporting information), the **XL** dyes exhibit similar electron distribution in the frontier orbitals. The HOMOs are delocalized mainly over the phenothiazine donor, the neighboring π spacer and the auxiliary benzothiadiazole acceptor. Whereas, the LUMOs are distributed mainly from the acceptor to the benzothiadiazole moiety. For the isomeric dyes **XL1** and **XL2**, the latter exhibits better overlapping between the HOMO and LUMO electrons with respect to the former, demonstrating that the HT unit neighboring to the acceptor terminal is favorable for the charge transfer and injection of the excited electrons into the TiO_2 semiconductor. With respect to the optimized geometry, the dihedral angles between the HT and benzothiadiazole units are smaller than 15°, irrespective of the position of the HT unit. On the other hand, the angles between the donors and the adjacent units increase in the order of **XL2** (31.58°) < **XL3** (41.86°) ≈ **XL1** (42.01°), indicating that the steric hindrance associated with the hexyl chain on the HT unit and the neighboring phenothiazine donor can raise the dihedral angle between them, and thus the more severe distortion could interrupt the conjugation, resulting in weakened intramolecular charge transfer (ICT) effect. This structural feature leads to the

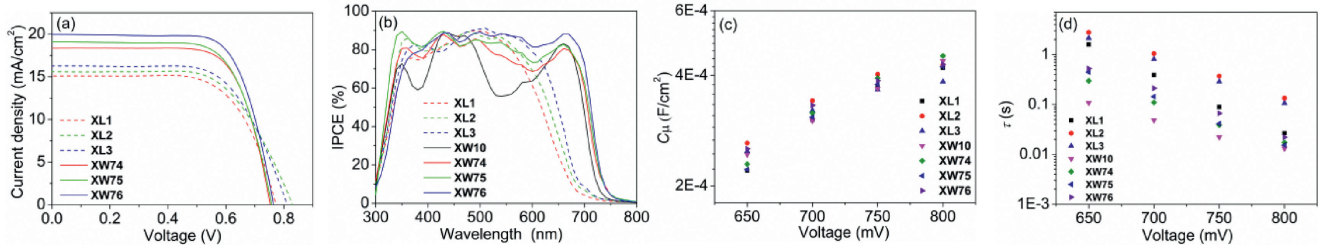

Fig. 3. (a) *J*–*V* characteristic curves, (b) IPCE spectra, plots of (c) C_μ and (d) τ *versus* the bias voltages of the DSSCs based on the sensitizers.

Table 1
Photovoltaic performance of DSSCs based on **XL1**-**XL3, XW74**-**XW76** and the reference dye **XW10**.[a]

Dyes	V_{OC} (mV)	J_{SC} (mA/cm^2)	FF (%)	PCE (%)
XL1	776 ± 2	15.09 ± 0.31	67.41 ± 0.66	7.89 ± 0.14
XL2	819 ± 5	15.50 ± 0.14	64.53 ± 0.39	8.19 ± 0.13
XL3	810 ± 3	16.31 ± 0.16	65.81 ± 0.24	8.69 ± 0.07
XW74	752 ± 3	18.56 ± 0.16	70.29 ± 0.69	9.81 ± 0.06
XW75	754 ± 2	19.24 ± 0.33	69.62 ± 0.46	10.10 ± 0.21
XW76	765 ± 5	19.94 ± 0.18	70.70 ± 0.66	10.78 ± 0.11
XW76[b]	768 ± 3	20.19 ± 0.21	70.94 ± 1.11	10.99 ± 0.14
XW76[c]	772 ± 2	20.48 ± 0.26	71.74 ± 0.47	11.35 ± 0.07
XW76[d]	774 ± 4	19.53 ± 0.30	72.16 ± 0.30	10.91 ± 0.21
XW10	711 ± 5	17.90 ± 0.04	68.4 ± 0.5	8.6 ± 0.1 [20]

[a] The data were collected from three parallel cells (average values and errors). The TiO_2 electrode was dipped in the dye bath without CDCA.
[b] 0.5 mmol/L CDCA was added in the dye bath.
[c] 1.0 mmol/L CDCA was added in the dye bath.
[d] 1.5 mmol/L CDCA was added in the dye bath.

observed blue shift of the ICT band of **XL1**, consistent with the hypsochromically shifted absorption spectrum of **XL1** with respect to that of **XL2**.

To evaluate the photovoltaic behavior of the **XL** series dyes, they have been utilized in fabrication of DSSCs using the I^-/I_3^- electrolyte (see Supporting information for more details). The *J*-*V* curves (Fig. 3a) and IPCE spectra (Fig. 3b) were studied under AM 1.5 global sunlight and the corresponding photovoltaic parameters are collected in Table 1. The solar cells based on **XL1** afford the J_{SC}, V_{OC}, and PCE of 15.09 mA/cm^2, 776 mV, and 7.89%, respectively, and **XL2** exhibits an improved J_{SC} of 15.50 mA/cm^2, which may be ascribed to the red-shifted absorption and better overlapping between the HOMO and LUMO orbitals as indicated by the theoretical calculations (*vide supra*). Meanwhile, **XL2** exhibits an improved V_{OC} of 819 mV, which is among the highest V_{OC} values achieved for the DSSCs based on the iodine electrolyte [18,43,44]. The extraordinary V_{OC} value may be ascribed to the well balanced anti-aggregation ability around both the donor and the acceptor [45]. As a result of the improved J_{SC}, V_{OC}, an improved PCE of 8.19% was achieved for **XL2**. Compared with **XL2, XL3** affords a similar V_{OC}, accompanied with a dramatically enhanced J_{SC} of 16.31 mA/cm^2, which may be ascribed to the stronger light-harvesting capability as a consequence of the larger conjugated skeleton. Finally, **XL3** affords a highest PCE of 8.69% among the **XL** series of dyes, which may be ascribed to its most extensive absorption wavelength range as well as its highest molar extinction coefficient (*vide supra*), in spite of its smallest adsorption amount (Table S3 in Supporting information). To further understand the trend for the photocurrents, the incident photon-to-current conversion efficiency (IPCE) spectra have been recorded. As depicted in Fig. 3b, **XL1**–**XL3** display similar high IPCE plateaus exceeding 85% around 500 nm, with the band edges gradually extended in the sequence of **XL1** < **XL2** < **XL3**, consistent with that of the increasing J_{SC} values.

Coadsorption of **XL1**–**XL3** with various concentrations of CDCA was also investigated (Table S4 in Supporting information) to check the possibility of further improving the V_{OC} by reducing the dye-aggregation [46]. However, lowered V_{OC}, J_{SC} and PCE values were obtained in the presence of CDCA. The decreased V_{OC} values indicate that the inherent excellent anti-aggregation ability of the **XL**-sensitizers cannot be further improved by using CDCA, and the lowered J_{SC} values may be attributed to the decrease in the dye loading amounts due to the competitive adsorption of CDCA [24].

On this basis, we continued to check the photovoltaic behavior of the CC dyes **XW74**–**XW76**, which contain both the organic dye units of **XL1**–**XL3** and a porphyrin dye unit of **XW10** [20]. As a result, higher IPCE plateaus over the 300 nm to 700 nm range and higher J_{SC} values in the sequence of **XW74** (18.56 mA/cm^2) < **XW75** (19.24 mA/cm^2) < **XW76** (19.94 mA/cm^2) have been achieved. This trend is consistent with that obtained for the corresponding organic dye components (**XL1** < **XL2** < **XL3**). The J_{SC} values obtained for the CC dyes are dramatically higher than that obtained for **XW10**, which may be related to the panchromatic absorption character and high charge collection efficiencies (η_{cc}) for the CC dyes (Table S6 in Supporting information). Because of the contribution by the high V_{OC} values of the **XL1**–**XL3** components, the CC dyes exhibit V_{OC} values higher than that of the porphyrin component **XW10** [20] by at least 40 mV, with a highest V_{OC} of 765 mV achieved for **XW76**. As a result of the highest V_{OC} and J_{SC}, a highest PCE of 10.78% has been achieved for **XW76**. Despite the relatively high PCE, the obtained V_{OC} still needs to be further improved. Thus, coadsorption of **XW76** with various concentrations of CDCA was explored. Upon addition of CDCA, gradual improvement of V_{OC} is observed. However, excessive CDCA will compete with the sensitizer on the TiO_2 film, leading to decreased dye loading amount and lowered J_{SC}. Finally, by using an optimal concentration of 1.0 mmol/L CDCA, the best cell performance has been achieved with the V_{OC}, J_{SC}, and PCE of 772 mV, 20.48 mA/cm^2, and 11.35%, respectively. The relative deviations between the J_{SC} values obtained from the *J*-*V* tests and the integral ones obtained from the corresponding IPCE spectra lie within the range of 7%–12% (Table S5 and Figs. S5 and S6 in Supporting information). This disagreement may be ascribed to the fact that more electrons and heat generated in the full irradiation applied in the *J*-*V* test endow higher charge transport and collection efficiencies, and thus higher J_{SC} values were obtained in the *J*-*V* tests. By contrast, such effects are not so obvious in the monochromatic IPCE measurement [47].

With the purpose of revealing the factors affecting the V_{OC} values, electrochemical impedance characteristics under the dark condition have been monitored (Fig. S8 in Supporting information). The charge transport resistance (R_{tr}) and charge recombination resistance (R_{rec}) at a bias potential of −0.75 V are summarized in Table S6 (Supporting information), and the plots of chemical capacitances (C_μ) and electron lifetimes (τ) *versus* the bias voltages are shown in Figs. 3c and d. The results indicate that the R_{tr} values are comparable for all the dyes (9.94~15.28 Ω). By contrast, the R_{rec} values are dramatically different and positively related to

the V_{OC} values. Theoretically, for a certain electrolyte, the *quasi*-Fermi level of the TiO_2 semiconductor, which is associated with the conduction band edge level (*Ec*) and the free electron density, is a key factor affecting the V_{OC} [48]. As presented in Fig. 3c, the *Ec*-related C_μ values exhibit slight difference for all the dyes, indicative of the negligible effect of the conduction band shift on the V_{OC}. By contrast, the τ values, which are related positively to the free electron density in the TiO_2 films, raise in the order of **XW10** < **XW74** ≈ **XW75** < **XW76** < **XL1** < **XL3** < **XL2** at a fixed bias voltage, coinciding with the trend of increasing V_{OC} (Table 1). These results demonstrate that the V_{OC} values are dominated by the densities of the free electrons for these dyes, as revealed by the trends observed for R_{rec} and τ. Impressively, the DSSCs sensitized with **XL2** and **XL3** exhibit marvelous τ values which are roughly an order of magnitude higher than the corresponding values for the other dyes, consistent with the extraordinary V_{OC} values of 819 and 810 mV, respectively. These results further reveal that the presence of an HT unit close to the acceptor terminal can effectively suppress molecular aggregation and charge recombination, thus improving the free electron density and elongating the electron lifetime.

Photostability is a crucial factor for practical applications of DSSCs [49]. In this work, the long-term photovoltaic performance of the DSSCs soaked in visible light was monitored to evaluate the photostability. After 500 h of visible light soaking, the representative cells sensitized by **XL3** and **XW76** afforded efficiencies of 7.75% and 10.04%, which are 89% and 93% of the initial PCEs, respectively (Fig. S9 in Supporting information), further confirming that the DSSCs based on the CC dyes comprising two anchor groups display superior photostability with respect to those based on the single-anchor ones.

In summary, three metal-free organic sensitizers **XL1**–**XL3**, featured with different numbers and positions of β-hexylthiophene units and a benzothiadiazole unit, have been synthesized and used as the organic components for covalently linking with a porphyrin dye **XW10** to construct the corresponding CC dyes **XW74**–**XW76**. Notably, **XL2** with the β-hexylthiophene near the acceptor side affords a striking V_{OC} of 819 mV because of its superior anti-aggregation effect. Dye **XL3** comprising two HT groups on both sides of the benzothiadiazole unit not only shows intensified absorption bands in the green light region but also maintains the excellent anti-aggregation capability to give a relatively high V_{OC} (810 mV). On this basis, the corresponding CC dyes show enhanced J_{SC} values compared to **XW10** because of their panchromatic absorption behavior. Among them, **XW76** contains the **XL3** subunit, which exhibits the best photovoltaic behavior among the **XL** series of dyes as well as the most complementary absorption with **XW10**, affording the highest PCE of 10.78%. Coadsorption of **XW76** with CDCA affords a further improved PCE of 11.35%, which outperforms the previous intermolecular cosensitization system of **XW10**+**WS-5** (11.0%) [20]. These results illustrate the importance of tailoring the position and number of π spacers in designing high-performance organic dyes, which can be used as components for further linking with a porphyrin dye unit to construct CC dyes for fabricating efficient DSSCs.

Declaration of competing interest

The authors declare that they have no known competing financial interests or personal relationships that could have appeared to influence the work reported in this paper.

Acknowledgments

This work was financially supported by the National Natural Science Foundation of China (Nos. 22131005, 21772041, 21971063 and 22075077), the Program of Shanghai Academic Research Leader (No. 20XD1401400), the Natural Science Foundation of Shanghai (No. 20ZR1414100), and the Fundamental Research Funds for the Central Universities (No. 222201717003).

Supplementary materials

Supplementary material associated with this article can be found, in the online version, at doi:10.1016/j.cclet.2022.01.052.

References

[1] B. O'Regan, M. Grätzel, Nature 353 (1991) 737–740.
[2] A. Yella, H. Lee, H.N. Tsao, et al., Science 334 (2011) 629–634.
[3] S. Mathew, A. Yella, P. Gao, et al., Nat. Chem. 6 (2014) 242–247.
[4] K. Hu, R.N. Sampaio, J. Schneider, et al., J. Am. Chem. Soc. 142 (2020) 16099–16116.
[5] K. Zeng, Z. Tong, L. Ma, et al., Energy Environ. Sci. 13 (2020) 1617–1657.
[6] H. Rui, J. Shen, Z. Yu, et al., Angew. Chem. Int. Ed. 60 (2021) 16156–16163.
[7] J. Moutet, J.M. Veleta, T.L. Gianetti, ACS Appl. Energy Mater. 4 (2021) 9–14.
[8] M. Kokkonen, P. Talebi, J. Zhou, et al., J. Mater. Chem. A 9 (2021) 10527–10545.
[9] S. Song, J. Lu, W. Ye, et al., Sci. China Chem. 64 (2021) 1441–1459.
[10] B. Pashaei, H. Shahroosvand, M. Grätzel, et al., Chem. Rev. 116 (2016) 9485–9564.
[11] H. Jiang, Y. Ren, W. Zhang, et al., Angew. Chem. Int. Ed. 59 (2020) 9324–9329.
[12] T. Hua, Z. Huang, K. Cai, et al., Electrochim. Acta 302 (2019) 225–233.
[13] C. Liao, K. Zeng, H. Wu, et al., Cell Rep. Phys. Sci. 2 (2021) 100326.
[14] K. Zeng, Y. Chen, W. Zhu, et al., J. Am. Chem. Soc. 142 (2020) 5154–5161.
[15] K. Zeng, Y. Lu, W. Tang, et al., Chem. Sci. 10 (2019) 2186–2192.
[16] M. Yan, Q. Wang, Y. Zhu, et al., J. Photochem. Photobiol. A 416 (2021) 113325.
[17] H. Jia, Z. Ju, H. Sun, et al., J. Mater. Chem. A 2 (2014) 20841–20848.
[18] H. Jia, M. Zhang, W. Yan, et al., J. Mater. Chem. A 4 (2016) 11782–11788.
[19] K. Kakiage, Y. Aoyama, T. Yano, et al., Chem. Commun. 51 (2015) 15894–15897.
[20] Y. Xie, Y. Tang, W. Wu, et al., J. Am. Chem. Soc. 137 (2015) 14055–14058.
[21] Y. Lu, Y. Cheng, C. Li, et al., Sci. China. Chem. 62 (2019) 994.
[22] J. Ji, H. Zhou, Y.K. Eom, et al., Adv. Energy Mater. 10 (2020) 2000124.
[23] L. Zhang, X. Yang, W. Wang, et al., ACS Energy Lett. 4 (2019) 943–951.
[24] K. Zeng, W. Tang, C. Li, et al., J. Mater. Chem. A 7 (2019) 20854–20860.
[25] Y. Lu, H. Song, X. Li, et al., ACS Appl. Mater. Interfaces 11 (2019) 5046–5054.
[26] C. Li, J. Zhang, J. Song, et al., Sci. China Chem. 61 (2018) 511–514.
[27] H. Song, Q. Liu, Y. Xie, Chem. Commun. 54 (2018) 1811–1824.
[28] Y. Tang, X. Liu, Y. Wang, et al., Chin. Chem. Lett. 31 (2020) 1927–1930.
[29] S. Li, S. Zhang, S. Mei, et al., Dyes Pigm. 190 (2021) 109308.
[30] J.M. Cole, G. Pepe, O.K. Al Bahri, et al., Chem. Rev. 119 (2019) 7279–7327.
[31] J. Zou, Q. Yan, C. Li, et al., ACS Appl. Mater. Interfaces 12 (2020) 57017–57024.
[32] Y. Chen, Y. Tang, J. Zou, et al., ACS Appl. Mater. Interfaces 13 (2021) 49828–49839.
[33] P. Gao, H.N. Tsao, J. Teuscher, et al., Chin. Chem. Lett. 29 (2018) 289–292.
[34] N. Koumura, Z. Wang, S. Mori, et al., J. Am. Chem. Soc. 128 (2006) 14256–14257.
[35] Y. Wu, X. Zhang, W. Li, et al., Adv. Energy Mater. 2 (2012) 149–156.
[36] Z. Chai, J. Wang, Y. Xie, et al., ACS Appl. Mater. Interfaces 11 (2019) 27648–27657.
[37] M. Zhang, Y. Wang, M. Xu, et al., Energy Environ. Sci. 6 (2013) 2944–2949.
[38] J. Luo, Z. Wan, C. Jia, Chin. Chem. Lett. 27 (2016) 1304–1318.
[39] Z. Huang, H. Meier, D. Cao, J. Mater. Chem. C 4 (2016) 2404–2426.
[40] Y. Zhang, J. Song, J. Qu, et al., Sci. China Chem. 64 (2021) 341–357.
[41] C. Liao, H. Wu, Y. Fu, et al., Dyes Pigm. 194 (2021) 109582.
[42] A.D. Becke, J. Chem. Phys. 98 (1993) 5648–5652.
[43] R.Y. Lin, F. Wu, C. Li, et al., ChemSusChem 8 (2015) 2503–2513.
[44] M. Han, Y. Zhu, S. Liu, et al., J. Power Sources 387 (2018) 117–125.
[45] Z. Chai, M. Wu, M. Fang, et al., Adv. Energy Mater. 5 (2015) 1500846.
[46] Y. Lu, Q. Liu, J. Luo, et al., ChemSusChem 12 (2019) 2802–2809.
[47] H. Song, J. Zhang, J. Jin, et al., J. Mater. Chem. C 6 (2018) 3927–3936.
[48] H. Wu, J. Zhang, Y. Ren, et al., ACS Appl. Energy Mater. 3 (2020) 4549–4558.
[49] N. Yan, C. Zhao, S. You, et al., Chin. Chem. Lett. 31 (2020) 643–653.